

## Supporting Information

### Identification and In-Silico Binding Study of a Highly Potent DENV NS2B-NS3 Covalent Inhibitor

Xincheng Lin<sup>abc</sup>, Jiawei Cheng<sup>abc</sup>, Yuming Wu<sup>d</sup>, Yaoliang Zhang<sup>abc</sup>, Hailun Jiang<sup>abc</sup>, Jian Wang<sup>abc,\*</sup>, Xuejun

Wang<sup>d,\*</sup>, Maosheng Cheng<sup>abc,\*</sup>

<sup>a</sup> Key Laboratory of Structure-Based Drug Design & Discovery of Ministry of Education, Shenyang

Pharmaceutical University, Shenyang 110016, China

<sup>b</sup> School of Pharmaceutical Engineering, Shenyang Pharmaceutical University, Shenyang 110016, China

<sup>c</sup> Key Laboratory of Intelligent Drug Design and New Drug Discovery of Liaoning Province, Shenyang

Pharmaceutical University, Shenyang 110016, China

<sup>d</sup> Department of Biotechnology, Beijing Institute of Radiation Medicine, Beijing 100850, China

#### Table of contents:

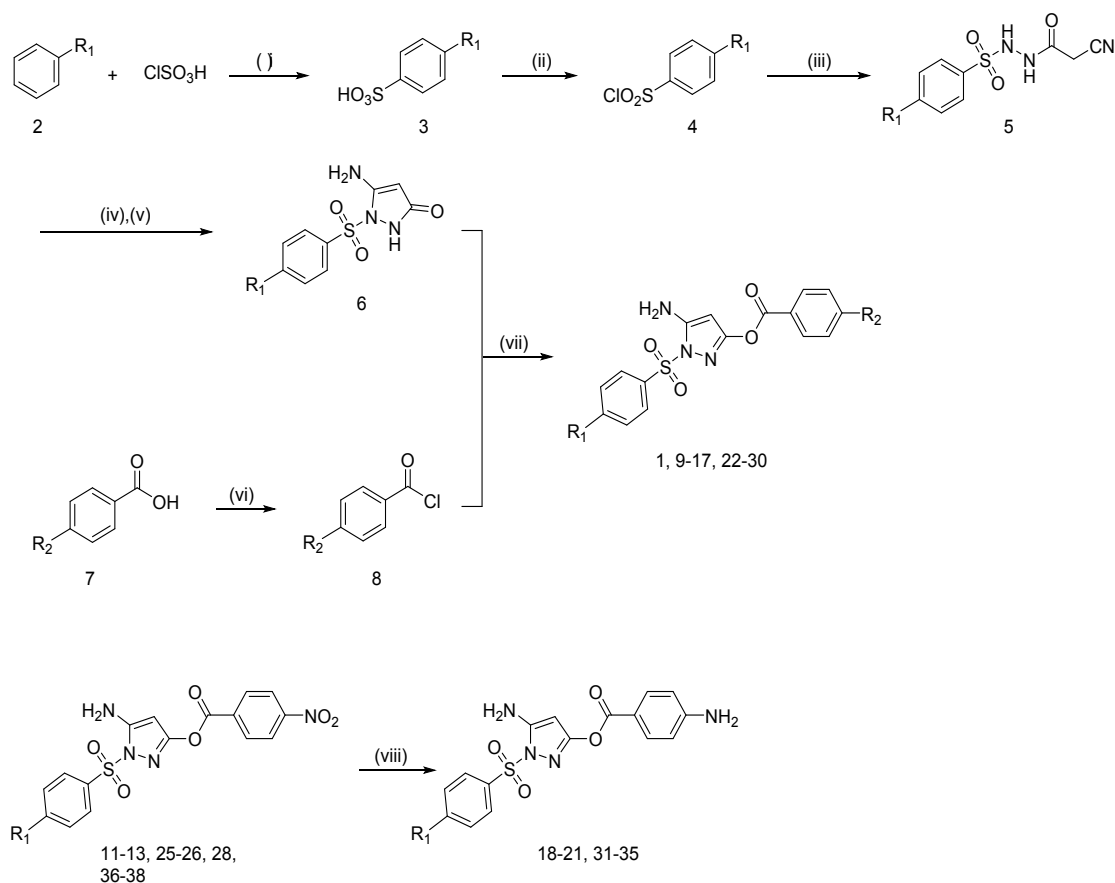
1. Chemistry .....	S2
2. Stability assay of compound .....	S9
3. Biology .....	S10
4. Computational analyses .....	S12
5. Supplementary Figures .....	S13
6. References: .....	S20

## 1. Chemistry

### 1.1 General chemistry

Commercially available solvents and reagents were used directly without further purification. Air-sensitive reactions were conducted under nitrogen protection. Silica gel H60 (200-300 mesh) for chromatography was purchased from Qingdao Haiyang Chemical Co., Ltd, silica gel 60 GF254 and UV light were used for TLC. MS data were obtained on Agilent 6120 Single Quadrupole LC/MS system equipped with photodiode array detector using electron spray ionization (ESI). NMR spectra were recorded on Bruker AVANCE III HD (5–650 MHz) spectrometer. DMSO-*d*<sub>6</sub> and Tetramethylsilane (TMS) were used as the solvent and internal reference for all NMR spectra.

**Scheme S1.** General Synthesis for Compounds <sup>a</sup>



<sup>a</sup> Reagents and conditions: (i) DCM, 0 °C, 4 h; (ii)  $\text{SOCl}_2$ , DMF (cat.), DCM, reflux for 6 h; (iii) Cyanoacetohydrazide, EtOH, r.t., 2 h; (iv) 1 M  $\text{NaOH}$ (aq.), r.t., 30 min; (v) 3 M  $\text{HCl}$ (aq.), r.t., 10 min; (vi)  $\text{SOCl}_2$ , DMF (cat.), DCM, reflux for 2 h; (vii)  $\text{DIPEA}$ , DCM, r.t., 10 h, (viii)  $\text{H}_2$ ,  $\text{Pd/C}$ , ethyl acetate, r.t., 12 h.

### 1.2 General synthetic procedure for intermediate 6

Solution of monosubstituted benzene intermediate 2 (30 mmol, 1.0 equiv) in dried DCM (20 mL) was cooled to 0°C. To this solution, another solution of chlorosulphonic acid (31.5 mmol, 1.05 equiv) in dried DCM (20 mL) was added dropwise, then stirred at 0°C for 4 h. After the reaction was completed, the reaction mixture was concentrated under vacuum to give p-substituted benzenesulfonic acid intermediate 3 (yield: 84-89%) as pink solid, which was used without purification in the next reaction.

A solution of p-substituted benzenesulfonic acid intermediate 3 (10 mmol, 1.0 equiv) in dried DCM (40 mL) was cooled to 0°C. To this solution thionyl chloride 4.353 mL (60 mmol, 6.0 equiv) and DMF two drops were added and warmed to r.t. and heated to gentle reflux for 6 h. The reaction mixture was cooled, concentrated under vacuum, and dried to give p-substituted benzenesulfonyl chloride intermediate 4 (yield: 89-91%) as solid, which was used without purification in the next reaction.

To a solution of p-substituted benzenesulfonyl chloride intermediate 4 (11.09 mmol, 1.1 equiv) in EtOH (50 mL) was added cyanoacetohydrazide 1.00 g (10.09 mmol, 1.0 equiv), then stirred at room temperature for 2 h. The reaction mixture was filtered and dried to give sulfonamide intermediate 5 (yield: 48-55%) as white solid, which was used without purification in the next reaction.

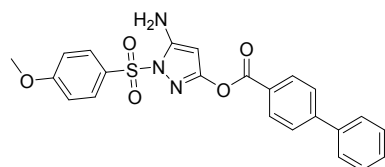
Sulfonamide intermediate 5 (5 mmol, 1.0 equiv) was added to 1 mol/L NaOH solution (15 mL, 15 mmol, 3.0 equiv). The reaction mixture was stirred at room temperature for 30 min. After adjusting the pH of the solution to 3 with 3 M HCl, the reaction mixture was filtrated, washed with water, and dried to give intermediate 6 (yield: 75-88%) as white solid, which was used without purification in the next reaction.

### 1.3 General synthetic procedure for commercially unavailable intermediate 8

A solution of p-substituted benzoic acid intermediate 7 (10 mmol, 1.0 equiv) in dried DCM (40 mL) was cooled to 0°C. To this solution thionyl chloride 4.353 mL (60 mmol, 6.0 equiv) and DMF 2 drops were added and heated to gentle reflux for 6 h. The reaction mixture was cooled, concentrated under vacuum, and dried to give p-substituted benzoyl chloride intermediate 8 (yield: 89-91%) as white solid, which was used without purification in the next reaction.

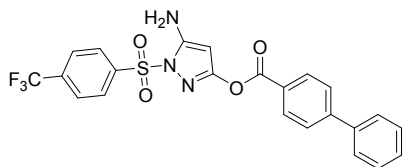
### 1.4 General synthetic procedure for 1, 9-17, 22-30, 36-38

To a solution of intermediate 6 (1.0 mmol, 1.0 equiv) in DCM (20 mL) was added p-substituted benzoyl chloride intermediate 8 (1.2 mmol, 1.2 equiv) and DIPEA 265  $\mu$ L (1.5 mmol, 1.5 equiv). The reaction mixture was stirred at room temperature for 10 h. After the reaction was completed, 2 M HCl (40 mL) was added to the solution and stirred for 5 min. Organic layers were separated, washed with water and brine, then dried over anhydrous Na<sub>2</sub>SO<sub>4</sub>, filtered, and concentrated under vacuum. The residue was purified by column chromatography (silica gel, PE/EA) to give products (yield: 57-76%) as solid.

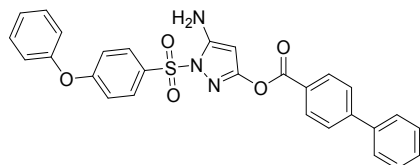


#### 5-amino-1-((4-methoxyphenyl)sulfonyl)-1H-pyrazol-3-yl [1,1'-biphenyl]-4-carboxylate (1).

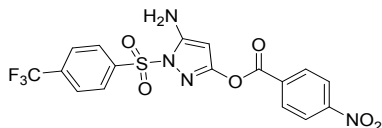
76.21% yield, m.p. 175.1-176.3°C, ESI-MS  $m/z$ : 450.1  $[M+H]^+$ , <sup>1</sup>H NMR (600 MHz, DMSO-*d*<sub>6</sub>)  $\delta$  8.15 – 8.07 (m, 2H), 7.93 – 7.86 (m, 4H), 7.79 – 7.74 (m, 2H), 7.52 (dd,  $J$  = 8.3, 6.8 Hz, 2H), 7.46 (d,  $J$  = 7.4 Hz, 1H), 7.24 – 7.14 (m, 2H), 6.52 (s, 2H), 5.37 (s, 1H), 3.86 (s, 3H), <sup>13</sup>C NMR (150 MHz, DMSO-*d*<sub>6</sub>)  $\delta$  164.07, 162.46, 158.63, 152.21, 145.77, 138.52, 130.61, 129.85, 129.16, 128.69, 127.84, 127.22, 127.08, 126.56, 115.00, 80.49, 55.94.



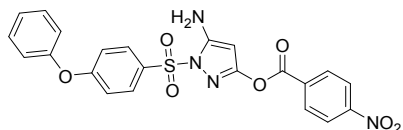
**5-amino-1-((4-(trifluoromethyl)phenyl)sulfonyl)-1H-pyrazol-3-yl [1,1'-biphenyl]-4-carboxylate (9).** 67.21% yield, m.p.194.2-195.7°C,ESI-MS  $m/z$ :488.1  $[M+H]^+$ ,  $^1H$  NMR (600 MHz, DMSO- $d_6$ )  $\delta$  8.18 (d,  $J$  = 8.3 Hz, 2H), 8.12 – 8.09 (m, 4H), 7.91 – 7.87 (m, 2H), 7.79 – 7.75 (m, 2H), 7.52 (dd,  $J$  = 8.4, 7.0 Hz, 2H), 7.50 – 7.42 (m, 1H), 6.67 (s, 2H), 5.42 (s, 1H),  $^{13}C$  NMR (150 MHz, DMSO- $d_6$ )  $\delta$  162.36, 159.57, 152.86, 145.83, 140.13, 138.49, 134.19 (q,  $J$  = 32.7 Hz), 130.64, 129.16, 128.70, 128.44, 127.22, 127.14 (d,  $J$  = 3.9 Hz), 127.08, 126.43, 125.90 – 120.38 (m), 80.93.



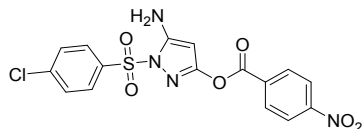
**5-amino-1-((4-phenoxyphenyl)sulfonyl)-1H-pyrazol-3-yl [1,1'-biphenyl]-4-carboxylate (10).** 71.34% yield, m.p.168.8-170.1°C,ESI-MS  $m/z$ :512.2  $[M+H]^+$ ,  $^1H$  NMR (600 MHz, DMSO- $d_6$ )  $\delta$  8.14 – 8.10 (m, 2H), 7.98 – 7.94 (m, 2H), 7.91 – 7.88 (m, 2H), 7.79 – 7.76 (m, 2H), 7.54 – 7.44 (m, 5H), 7.31 – 7.27 (m, 1H), 7.21 – 7.18 (m, 2H), 7.18 – 7.13 (m, 2H), 6.55 (s, 2H), 5.40 (s, 1H),  $^{13}C$  NMR (150 MHz, DMSO- $d_6$ )  $\delta$  162.57, 162.46, 158.78, 154.08, 152.29, 145.79, 138.51, 130.62, 130.52, 130.25, 129.89, 129.16, 128.70, 127.22, 127.08, 126.54, 125.50, 120.60, 117.54, 80.59.



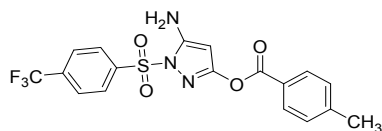
**5-amino-1-((4-(trifluoromethyl)phenyl)sulfonyl)-1H-pyrazol-3-yl 4-nitrobenzoate (11).** 63.14% yield, m.p.200.3-201.8°C,ESI-MS  $m/z$ :457.0  $[M+H]^+$ ,  $^1H$  NMR (600 MHz, DMSO- $d_6$ )  $\delta$  8.40 – 8.36 (m, 2H), 8.28 – 8.25 (m, 2H), 8.17 (d,  $J$  = 8.3 Hz, 2H), 8.10 (d,  $J$  = 8.5 Hz, 2H), 6.70 (s, 2H), 5.44 (s, 1H),  $^{13}C$  NMR (150 MHz, DMSO- $d_6$ )  $\delta$  161.12, 159.20, 152.89, 152.83, 150.79, 140.08, 134.23 (q,  $J$  = 32.7 Hz), 133.26, 131.47, 128.45, 127.13 (q,  $J$  = 3.7 Hz), 124.04, 125.85-120.41(m), 80.72.



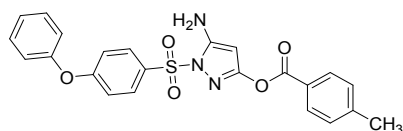
**5-amino-1-((4-phenoxyphenyl)sulfonyl)-1H-pyrazol-3-yl 4-nitrobenzoate (12).** 71.44% yield, m.p.176.8-178.2°C,ESI-MS  $m/z$ :503.0  $[M+Na]^+$ ,  $^1H$  NMR (600 MHz, DMSO- $d_6$ )  $\delta$  8.40 – 8.36 (m, 2H), 8.30 – 8.26 (m, 2H), 7.98 – 7.93 (m, 2H), 7.51 – 7.45 (m, 2H), 7.32 – 7.28 (m, 1H), 7.21 – 7.12 (m, 4H), 6.57 (s, 2H), 5.42 (s, 1H),  $^{13}C$  NMR (150 MHz, DMSO- $d_6$ )  $\delta$  162.61, 161.22, 158.42, 154.06, 152.32, 150.78, 133.35, 131.46, 130.53, 130.26, 129.82, 125.52, 124.05, 120.60, 117.55, 80.38.



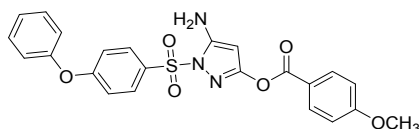
**5-amino-1-((4-chlorophenyl)sulfonyl)-1H-pyrazol-3-yl 4-nitrobenzoate (13).** 59.96% yield, m.p.163.0-163.5°C,ESI-MS  $m/z$ :423.0  $[M+H]^+$ ,  $^1H$  NMR (600 MHz, DMSO- $d_6$ )  $\delta$  8.40 – 8.36 (m, 2H), 8.29 – 8.26 (m, 2H), 7.97 – 7.95 (m, 2H), 7.80 – 7.77 (m, 2H), 6.64 (s, 2H), 5.43 (s, 1H),  $^{13}C$  NMR (150 MHz, DMSO- $d_6$ )  $\delta$  161.16, 158.93, 152.71, 150.78, 140.10, 135.12, 133.29, 131.46, 130.06, 129.29, 124.04, 80.59.



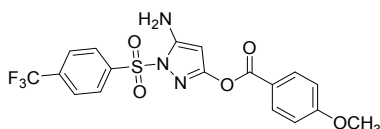
**5-amino-1-((4-(trifluoromethyl)phenyl)sulfonyl)-1H-pyrazol-3-yl 4-methylbenzoate (14).** 59.27% yield, m.p.182.3-184.0°C,ESI-MS  $m/z$ :426.1  $[M+H]^+$ ,  $^1H$  NMR (600 MHz, DMSO- $d_6$ )  $\delta$  8.16 (d,  $J$  = 8.3 Hz, 2H), 8.09 (d,  $J$  = 8.4 Hz, 2H), 7.95 – 7.90 (m, 2H), 7.39 (d,  $J$  = 8.1 Hz, 2H), 6.63 (s, 2H), 5.38 (s, 1H), 2.40 (s, 3H),  $^{13}C$  NMR (150 MHz, DMSO- $d_6$ )  $\delta$  162.55, 159.63, 152.86, 145.28, 140.15, 134.22 (q,  $J$  = 32.4, 31.9 Hz), 130.03, 129.71, 129.51, 128.46, 127.14 (d,  $J$  = 4.0 Hz), 123.17 (d,  $J$  = 273.1 Hz), 122.26, 114.82, 80.99, 21.30.



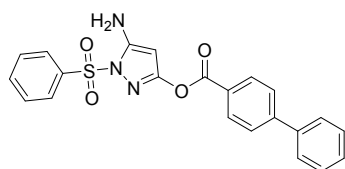
**5-amino-1-((4-phenoxyphenyl)sulfonyl)-1H-pyrazol-3-yl 4-methylbenzoate (15).** 62.45% yield, m.p.157.2-158.1°C,ESI-MS  $m/z$ :450.1  $[M+H]^+$ ,  $^1H$  NMR (600 MHz, DMSO- $d_6$ )  $\delta$  7.96 – 7.92 (m, 4H), 7.50 – 7.46 (m, 2H), 7.41 – 7.38 (m, 2H), 7.31 – 7.28 (m, 1H), 7.20 – 7.17 (m, 2H), 7.17 – 7.14 (m, 2H), 6.52 (s, 2H), 5.35 (s, 1H), 2.41 (s, 3H),  $^{13}C$  NMR (150 MHz, DMSO- $d_6$ )  $\delta$  162.61, 162.56, 158.80, 154.08, 152.26, 145.18, 130.52, 130.23, 129.97, 129.90, 129.67, 125.50, 124.98, 120.60, 117.53, 80.61, 21.27.



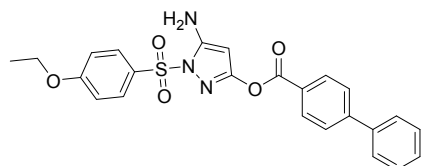
**5-amino-1-((4-phenoxyphenyl)sulfonyl)-1H-pyrazol-3-yl 4-methoxybenzoate (16).** 60.16% yield, m.p.150.1-151.2°C,ESI-MS  $m/z$ :466.1  $[M+H]^+$ ,  $^1H$  NMR (600 MHz, DMSO- $d_6$ )  $\delta$  8.02 – 7.98 (m, 2H), 7.96 – 7.92 (m, 2H), 7.50 – 7.46 (m, 2H), 7.31 – 7.27 (m, 1H), 7.21 – 7.17 (m, 2H), 7.17 – 7.13 (m, 2H), 7.12 – 7.08 (m, 2H), 6.51 (s, 2H), 5.34 (s, 1H), 3.86 (s, 3H),  $^{13}C$  NMR (150 MHz, DMSO- $d_6$ )  $\delta$  164.10, 162.54, 162.25, 158.89, 154.08, 152.23, 132.22, 130.52, 130.22, 129.92, 125.49, 120.59, 119.71, 117.52, 114.43, 80.66, 55.69.



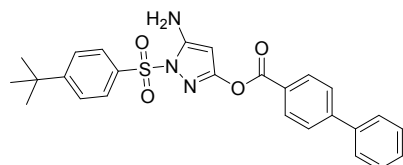
**5-amino-1-((4-(trifluoromethyl)phenyl)sulfonyl)-1H-pyrazol-3-yl 4-methoxybenzoate (17).** 63.76% yield, m.p.173.7-174.5°C,ESI-MS  $m/z$ :442.0  $[M+H]^+$ ,  $^1H$  NMR (600 MHz, DMSO- $d_6$ )  $\delta$  8.16 (d,  $J$  = 8.3 Hz, 2H), 8.09 (d,  $J$  = 8.4 Hz, 2H), 7.99 (d,  $J$  = 8.9 Hz, 2H), 7.10 (d,  $J$  = 8.9 Hz, 2H), 6.63 (s, 2H), 5.37 (s, 1H), 3.86 (s, 3H),  $^{13}C$  NMR (150 MHz, DMSO- $d_6$ )  $\delta$  164.14, 162.14, 159.67, 152.80, 140.14, 134.16 (q,  $J$  = 32.3 Hz) 132.25, 128.41, 127.17 – 127.01 (m), 123.14 (q,  $J$  = 273.2 Hz), 119.60, 114.44, 81.01, 55.70.



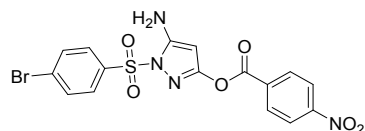
**5-amino-1-(phenylsulfonyl)-1H-pyrazol-3-yl [1,1'-biphenyl]-4-carboxylate (22).** 68.14% yield, m.p.170.5-171.7°C,ESI-MS  $m/z$ :420.1  $[M+H]^+$ ,  $^1H$  NMR (600 MHz, DMSO- $d_6$ )  $\delta$  8.13 – 8.10 (m, 2H), 7.98 – 7.95 (m, 2H), 7.90 – 7.88 (m, 2H), 7.82 – 7.79 (m, 1H), 7.78 – 7.75 (m, 2H), 7.71 – 7.68 (m, 2H), 7.52 (dd,  $J$  = 8.4, 6.9 Hz, 2H), 7.47 – 7.44 (m, 1H), 6.58 (s, 2H), 5.39 (s, 1H),  $^{13}C$  NMR (150 MHz, DMSO- $d_6$ )  $\delta$  162.64, 159.18, 152.73, 146.01, 138.73, 136.77, 135.17, 130.85, 130.04, 129.38, 128.91, 127.54, 127.43, 127.30, 126.73, 80.87.



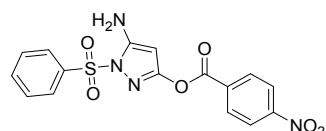
**5-amino-1-((4-ethoxyphenyl)sulfonyl)-1H-pyrazol-3-yl [1,1'-biphenyl]-4-carboxylate (23).** 72.77% yield, m.p.169.4-170.8°C,ESI-MS  $m/z$ :464.1  $[M+H]^+$ ,  $^1H$  NMR (600 MHz, DMSO- $d_6$ )  $\delta$  8.15 – 8.08 (m, 2H), 7.89 (t,  $J$  = 2.1 Hz, 2H), 7.88 (t,  $J$  = 2.2 Hz, 2H), 7.78 – 7.76 (m, 2H), 7.52 (dd,  $J$  = 8.4, 6.9 Hz, 2H), 7.47 – 7.43 (m, 1H), 7.19 – 7.15 (m, 2H), 6.52 (s, 2H), 5.37 (s, 1H), 4.14 (q,  $J$  = 7.0 Hz, 2H), 1.34 (t,  $J$  = 7.0 Hz, 3H),  $^{13}C$  NMR (150 MHz, DMSO- $d_6$ )  $\delta$  163.38, 162.46, 158.62, 152.21, 145.77, 138.51, 130.60, 129.86, 129.16, 128.69, 127.63, 127.21, 127.07, 126.56, 115.29, 80.48, 64.09, 14.35.



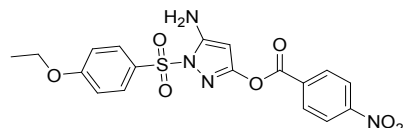
**5-amino-1-((4-tert-butylphenyl)sulfonyl)-1H-pyrazol-3-yl [1,1'-biphenyl]-4-carboxylate (24).** 66.17% yield, m.p.188.0-188.5°C,ESI-MS  $m/z$ :476.1  $[M+H]^+$ ,  $^1H$  NMR (600 MHz, DMSO- $d_6$ )  $\delta$  8.14 – 8.11 (m, 2H), 7.90 (dd,  $J$  = 3.4, 1.8 Hz, 2H), 7.89 (t,  $J$  = 2.5 Hz, 2H), 7.79 – 7.76 (m, 2H), 7.73 – 7.71 (m, 2H), 7.53 (dd,  $J$  = 8.3, 6.9 Hz, 2H), 7.47 – 7.44 (m, 1H), 6.56 (s, 2H), 5.40 (s, 1H), 1.30 (s, 9H),  $^{13}C$  NMR (150 MHz, DMSO- $d_6$ )  $\delta$  162.45, 158.67, 158.19, 152.23, 145.79, 138.51, 133.85, 130.62, 129.16, 128.69, 127.29, 127.22, 127.07, 126.76, 126.54, 80.54, 35.16, 30.61.



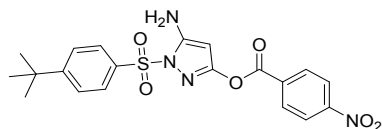
**5-amino-1-((4-bromophenyl)sulfonyl)-1H-pyrazol-3-yl 4-nitrobenzoate (25).** 61.32% yield, m.p.187.4-188.9°C,ESI-MS  $m/z$ :467.0  $[M+H]^+$ ,  $^1H$  NMR (600 MHz, DMSO- $d_6$ )  $\delta$  8.40 – 8.36 (m, 2H), 8.29 – 8.26 (m, 2H), 7.94 – 7.91 (m, 2H), 7.89 – 7.86 (m, 2H), 6.64 (s, 2H), 5.43 (s, 1H),  $^{13}C$  NMR (150 MHz, DMSO- $d_6$ )  $\delta$  161.15, 158.94, 152.71, 150.78, 135.54, 133.29, 133.00, 131.47, 129.30, 129.26, 124.04, 80.59.



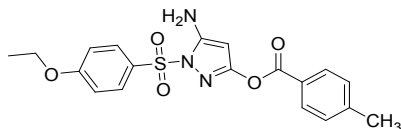
**5-amino-1-(phenylsulfonyl)-1H-pyrazol-3-yl 4-nitrobenzoate (26).** 64.77% yield, m.p.176.6-171.8°C,ESI-MS  $m/z$ :389.0  $[M+H]^+$ ,  $^1H$  NMR (600 MHz, DMSO- $d_6$ )  $\delta$  8.40 – 8.34 (m, 2H), 8.30 – 8.25 (m, 2H), 7.98 – 7.93 (m, 2H), 7.82 – 7.78 (m, 1H), 7.69 (t,  $J$  = 7.9 Hz, 2H), 6.61 (s, 2H), 5.41 (s, 1H),  $^{13}C$  NMR (150 MHz, DMSO- $d_6$ )  $\delta$  161.19, 158.60, 152.54, 150.77, 136.48, 134.99, 133.32, 131.46, 129.84, 127.32, 124.03, 80.44.



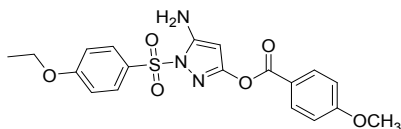
**5-amino-1-((4-ethoxyphenyl)sulfonyl)-1H-pyrazol-3-yl 4-nitrobenzoate (27).** 69.08% yield, m.p.175.5-176.7°C,ESI-MS  $m/z$ :433.1  $[M+H]^+$ ,  $^1H$  NMR (600 MHz, DMSO- $d_6$ )  $\delta$  8.42 – 8.31 (m, 2H), 8.31 – 8.24 (m, 2H), 7.90 – 7.84 (m, 2H), 7.19 – 7.15 (m, 2H), 6.55 (s, 2H), 5.39 (s, 1H), 4.14 (q,  $J$  = 7.0 Hz, 2H), 1.34 (t,  $J$  = 7.0 Hz, 3H),  $^{13}C$  NMR (150 MHz, DMSO- $d_6$ )  $\delta$  163.41, 161.22, 158.25, 152.22, 150.76, 133.36, 131.44, 129.87, 127.56, 124.04, 115.30, 80.27, 64.11, 14.34.



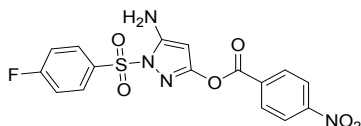
**5-amino-1-((4-(tert-butyl)phenyl)sulfonyl)-1H-pyrazol-3-yl 4-nitrobenzoate (28).** 58.84% yield, m.p.194.9-195.7°C,ESI-MS  $m/z$ :445.1  $[M+H]^+$ ,  $^1H$  NMR (600 MHz, DMSO- $d_6$ )  $\delta$  8.38 (d,  $J$  = 8.9 Hz, 2H), 8.28 (d,  $J$  = 9.0 Hz, 2H), 7.89 (d,  $J$  = 8.7 Hz, 2H), 7.72 (d,  $J$  = 8.7 Hz, 2H), 6.59 (s, 2H), 5.42 (s, 1H), 1.30 (s, 9H),  $^{13}C$  NMR (150 MHz, DMSO- $d_6$ )  $\delta$  161.21, 158.32, 158.25, 152.25, 150.77, 133.77, 133.35, 131.46, 127.30, 126.78, 124.04, 80.33, 35.16, 30.61.



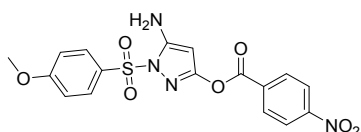
**5-amino-1-((4-ethoxyphenyl)sulfonyl)-1H-pyrazol-3-yl 4-methylbenzoate (29).** 63.17% yield, m.p.156.9-158.2°C,ESI-MS  $m/z$ :402.1  $[M+H]^+$ ,  $^1H$  NMR (600 MHz, DMSO- $d_6$ )  $\delta$  7.98 – 7.91 (m, 2H), 7.90 – 7.83 (m, 2H), 7.39 (d,  $J$  = 8.0 Hz, 2H), 7.19 – 7.13 (m, 2H), 6.50 (s, 2H), 5.33 (s, 1H), 4.14 (q,  $J$  = 7.0 Hz, 2H), 2.40 (s, 3H), 1.34 (t,  $J$  = 7.0 Hz, 3H),  $^{13}C$  NMR (150 MHz, DMSO- $d_6$ )  $\delta$  163.36, 162.61, 158.63, 152.18, 145.15, 129.95, 129.83, 129.66, 127.63, 125.00, 115.28, 80.50, 64.08, 21.26, 14.35



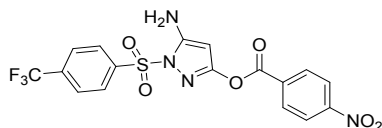
**5-amino-1-((4-ethoxyphenyl)sulfonyl)-1H-pyrazol-3-yl 4-methoxybenzoate (30).** 57.64% yield, m.p.149.2-150.1°C,ESI-MS  $m/z$ :418.1  $[M+H]^+$ ,  $^1H$  NMR (600 MHz, DMSO- $d_6$ )  $\delta$  8.00 – 7.98 (m, 2H), 7.88 – 7.85 (m, 2H), 7.17 – 7.15 (m, 2H), 7.11 – 7.08 (m, 2H), 6.49 (s, 2H), 5.32 (s, 1H), 4.13 (d,  $J$  = 7.0 Hz, 2H), 3.86 (s, 3H), 1.34 (t,  $J$  = 7.0 Hz, 3H),  $^{13}C$  NMR (150 MHz, DMSO- $d_6$ )  $\delta$  164.08, 163.35, 162.25, 158.72, 152.14, 132.20, 129.83, 127.66, 119.74, 115.27, 114.42, 80.56, 64.08, 55.68, 14.34.



**5-amino-1-((4-fluorophenyl)sulfonyl)-1H-pyrazol-3-yl 4-nitrobenzoate (36).** 64.28% yield, m.p.185.5-186.2°C,ESI-MS  $m/z$ :407.0  $[M+H]^+$ ,  $^1H$  NMR (600 MHz, DMSO- $d_6$ )  $\delta$  8.41 – 8.35 (m, 2H), 8.30 – 8.25 (m, 2H), 8.08 – 8.02 (m, 2H), 7.55 (t,  $J$  = 8.8 Hz, 2H), 6.63 (s, 2H), 5.42 (s, 1H),  $^{13}C$  NMR (150 MHz, DMSO- $d_6$ )  $\delta$  166.42, 164.73, 161.17, 158.80, 152.61, 150.78, 133.30, 132.68 (d,  $J$  = 1.7 Hz), 131.46, 130.75 (d,  $J$  = 9.9 Hz), 124.04, 117.23 (d,  $J$  = 23.7 Hz), 80.53.



**5-amino-1-((4-methoxyphenyl)sulfonyl)-1H-pyrazol-3-yl 4-nitrobenzoate (37).** 58.19% yield, m.p.181.2-182.3°C,ESI-MS  $m/z$ :419.0  $[M+H]^+$ ,  $^1H$  NMR (600 MHz, DMSO- $d_6$ )  $\delta$  8.38 (d,  $J$  = 8.9 Hz, 2H), 8.27 (d,  $J$  = 8.9 Hz, 2H), 7.90 (d,  $J$  = 9.0 Hz, 2H), 7.19 (d,  $J$  = 9.0 Hz, 2H), 6.55 (s, 2H), 5.39 (s, 1H), 3.86 (s, 3H),  $^{13}C$  NMR (150 MHz, DMSO- $d_6$ )  $\delta$  164.10, 161.21, 158.26, 152.22, 150.76, 133.35, 131.43, 129.86, 127.76, 124.03, 115.00, 80.27, 55.95.

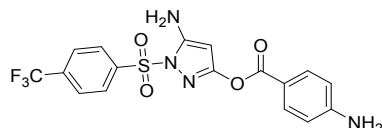


**5-amino-1-((4-(trifluoromethyl)phenyl)sulfonyl)-1H-pyrazol-3-yl 4-nitrobenzoate (38).** 63.14% yield, m.p.200.3-201.8°C,ESI-MS  $m/z$ :457.0  $[M+H]^+$ ,  $^1H$  NMR (600 MHz, DMSO- $d_6$ )  $\delta$  8.40 – 8.36 (m, 2H), 8.28 – 8.25 (m, 2H), 8.17 (d,  $J$  = 8.3 Hz, 2H), 8.10 (d,  $J$  = 8.5 Hz, 2H), 6.70 (s, 2H), 5.44 (s, 1H),

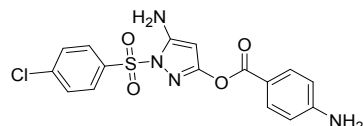
$^{13}\text{C}$  NMR (150 MHz,  $\text{DMSO}-d_6$ )  $\delta$  161.12, 159.20, 152.89, 152.83, 150.79, 140.08, 134.23 (q,  $J = 32.7$  Hz), 133.26, 131.47, 128.45, 127.13 (q,  $J = 3.7$  Hz), 124.04, 125.85-120.41(m), 80.72.

### 1.5 General synthetic procedure for 18-21, 31-35

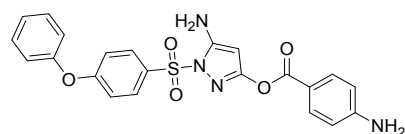
A solution of **11** 0.50 g in EA (30 mL) was added 0.05 g 10% Pd/C. The resulting mixture was stirred for 12 hours at room temperature under a balloon of hydrogen. After reaction completed, the suspension was filtered. The filtrate was concentrated under vacuum. The residue was purified by column chromatography (silica gel,  $\text{DCM}/\text{MeOH} = 20/1$  v/v) to give compound **18** (yield: 43.15 %) as solid. **19-21, 31-35** were prepared in a similar method by replacing **11** with the corresponding nitro compound from **12-13, 25-26, 28, 36-38**.



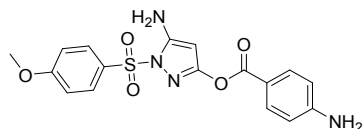
**5-amino-1-((4-(trifluoromethyl)phenyl)sulfonyl)-1H-pyrazol-3-yl 4-aminobenzoate (18).** 43.15% yield, m.p.197.1-198.4°C,ESI-MS  $m/z$ :427.1  $[\text{M}+\text{H}]^+$ ,  $^1\text{H}$  NMR (600 MHz,  $\text{DMSO}-d_6$ )  $\delta$  8.14 (d,  $J = 8.4$  Hz, 2H), 8.09 (d,  $J = 8.7$  Hz, 2H), 7.70 – 7.66 (m, 2H), 6.60 – 6.58 (m, 2H), 6.57 (s, 2H), 6.28 (s, 2H), 5.31 (s, 1H),  $^{13}\text{C}$  NMR (150 MHz,  $\text{DMSO}-d_6$ )  $\delta$  162.42, 160.11, 154.75, 152.68, 140.19, 134.10 (q,  $J = 32.6$  Hz), 132.19, 128.39, 127.06 (q,  $J = 3.7$  Hz), 125.87- 120.44(m), 112.82, 112.76, 81.20.



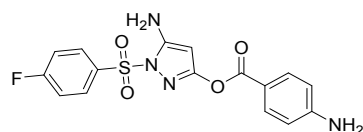
**5-amino-1-((4-chlorophenyl)sulfonyl)-1H-pyrazol-3-yl 4-aminobenzoate (19).** 43.12% yield, m.p.184.5-185.6°C,ESI-MS  $m/z$ :393.0  $[\text{M}+\text{H}]^+$ ,  $^1\text{H}$  NMR (600 MHz,  $\text{DMSO}-d_6$ )  $\delta$  7.95 – 7.92 (m, 2H), 7.78 – 7.75 (m, 2H), 7.71 – 7.67 (m, 2H), 6.61 – 6.58 (m, 2H), 6.52 (s, 2H), 6.28 (s, 2H), 5.29 (s, 1H),  $^{13}\text{C}$  NMR (150 MHz,  $\text{DMSO}-d_6$ )  $\delta$  159.86, 154.74, 152.52, 139.94, 135.23, 132.19, 129.99, 129.25, 112.83, 81.08.



**5-amino-1-((4-phenoxyphenyl)sulfonyl)-1H-pyrazol-3-yl 4-aminobenzoate (20).** 54.66% yield, m.p.174.5-175.7°C,ESI-MS  $m/z$ :451.1  $[\text{M}+\text{H}]^+$ ,  $^1\text{H}$  NMR (600 MHz,  $\text{DMSO}-d_6$ )  $\delta$  7.94 – 7.92 (m, 2H), 7.71 – 7.68 (m, 2H), 7.50 – 7.46 (m, 2H), 7.31 – 7.28 (m, 1H), 7.20 – 7.17 (m, 2H), 7.16 – 7.12 (m, 2H), 6.61 – 6.58 (m, 2H), 6.45 (s, 2H), 6.27 (s, 2H), 5.29 (s, 1H),  $^{13}\text{C}$  NMR (150 MHz,  $\text{DMSO}-d_6$ )  $\delta$  162.53, 162.48, 159.32, 154.70, 154.10, 152.12, 132.15, 130.51, 130.19, 129.99, 125.47, 120.60, 117.50, 112.91, 112.83, 80.86.



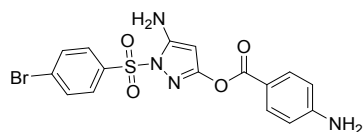
**5-amino-1-((4-methoxyphenyl)sulfonyl)-1H-pyrazol-3-yl 4-aminobenzoate (21).** 52.21% yield, m.p.178.1-179.9°C,ESI-MS  $m/z$ :389.1  $[\text{M}+\text{H}]^+$ ,  $^1\text{H}$  NMR (600 MHz,  $\text{DMSO}-d_6$ )  $\delta$  7.90 – 7.85 (m, 2H), 7.72 – 7.66 (m, 2H), 7.20 – 7.15 (m, 2H), 6.63 – 6.54 (m, 2H), 6.43 (s, 2H), 6.26 (s, 2H), 5.26 (s, 1H), 3.85 (s, 3H),  $^{13}\text{C}$  NMR (150 MHz,  $\text{DMSO}-d_6$ )  $\delta$  163.97, 162.53, 159.18, 154.68, 152.05, 132.13, 129.79, 127.93, 114.93, 112.95, 112.82, 80.76, 55.92.



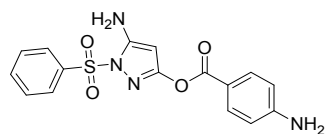
**5-amino-1-((4-fluorophenyl)sulfonyl)-1H-pyrazol-3-yl 4-aminobenzoate (31).** 46.58% yield,



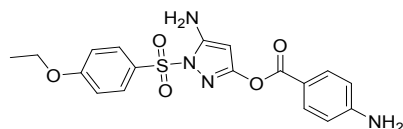
m.p.183.0-183.8°C,ESI-MS  $m/z$ :377.0  $[M+H]^+$ ,  $^1H$  NMR (600 MHz, DMSO- $d_6$ )  $\delta$  8.03 – 8.00 (m, 2H), 7.71 – 7.67 (m, 2H), 7.56 – 7.52 (m, 2H), 6.61 – 6.58 (m, 2H), 6.50 (s, 2H), 6.27 (s, 2H), 5.29 (s, 1H),  $^{13}C$  NMR (150 MHz, DMSO- $d_6$ )  $\delta$  166.31, 164.63, 162.48, 159.71, 154.72, 152.42, 132.81 (d,  $J$  = 2.7 Hz), 132.17, 130.67 (d,  $J$  = 9.9 Hz), 117.15 (d,  $J$  = 22.9 Hz), 112.85, 112.83, 81.02.



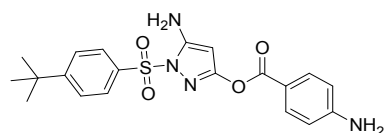
**5-amino-1-((4-bromophenyl)sulfonyl)-1H-pyrazol-3-yl 4-aminobenzoate (32).** 42.33% yield, m.p.185.7-186.8°C,ESI-MS  $m/z$ :437.0  $[M+H]^+$ ,  $^1H$  NMR (600 MHz, DMSO- $d_6$ )  $\delta$  7.93 – 7.89 (m, 2H), 7.85 (d,  $J$  = 8.7 Hz, 2H), 7.71 – 7.67 (m, 2H), 6.61 – 6.57 (m, 2H), 6.51 (s, 2H), 6.27 (s, 2H), 5.29 (s, 1H),  $^{13}C$  NMR (150 MHz, DMSO- $d_6$ )  $\delta$  162.45, 159.85, 154.73, 152.51, 135.65, 132.92, 132.18, 129.21, 129.12, 112.82, 81.07.



**5-amino-1-(phenylsulfonyl)-1H-pyrazol-3-yl 4-aminobenzoate (33).** 47.23% yield, m.p.174.5-175.9°C,ESI-MS  $m/z$ :359.0  $[M+H]^+$ ,  $^1H$  NMR (600 MHz, DMSO- $d_6$ )  $\delta$  7.95 – 7.92 (m, 2H), 7.78 (d,  $J$  = 7.6 Hz, 1H), 7.70 – 7.66 (m, 4H), 6.60 – 6.57 (m, 2H), 6.49 (s, 2H), 6.26 (s, 2H), 5.28 (s, 1H),  $^{13}C$  NMR (150 MHz, DMSO- $d_6$ )  $\delta$  162.50, 159.51, 154.70, 152.35, 136.62, 134.83, 132.16, 129.77, 127.27, 112.89, 112.82, 80.93.



**5-amino-1-((4-ethoxyphenyl)sulfonyl)-1H-pyrazol-3-yl 4-aminobenzoate (34).** 52.47% yield, m.p.172.5-173.3°C,ESI-MS  $m/z$ :403.1  $[M+H]^+$ ,  $^1H$  NMR (600 MHz, DMSO- $d_6$ )  $\delta$  8.00 – 7.98 (m, 2H), 7.88 – 7.85 (m, 2H), 7.17 – 7.15 (m, 2H), 7.11 – 7.08 (m, 2H), 6.49 (s, 2H), 5.32 (s, 1H), 4.13 (d,  $J$  = 7.0 Hz, 2H), 3.86 (s, 3H), 1.34 (t,  $J$  = 7.0 Hz, 3H),  $^{13}C$  NMR (150 MHz, DMSO- $d_6$ )  $\delta$  163.29, 162.53, 159.16, 154.68, 152.04, 132.13, 129.79, 127.72, 115.23, 112.95, 112.82, 80.75, 64.06, 14.35.



**5-amino-1-((4-(tert-butyl)phenyl)sulfonyl)-1H-pyrazol-3-yl 4-aminobenzoate (35).** 45.48% yield, m.p.191.6-192.7°C,ESI-MS  $m/z$ :415.1  $[M+H]^+$ ,  $^1H$  NMR (600 MHz, DMSO- $d_6$ )  $\delta$  7.87 – 7.85 (m, 2H), 7.70 (d,  $J$  = 3.2 Hz, 2H), 7.69 (d,  $J$  = 3.2 Hz, 2H), 6.61 – 6.58 (m, 2H), 6.46 (s, 2H), 6.26 (s, 2H), 5.29 (s, 1H), 1.29 (s, 9H),  $^{13}C$  NMR (150 MHz, DMSO- $d_6$ )  $\delta$  162.52, 159.20, 158.06, 154.70, 152.05, 133.92, 132.15, 127.24, 126.70, 112.90, 112.82, 80.80, 35.13, 30.61.

## 2. Stability assay of compound

In order to evaluate the stability of these compounds during enzymatic assays, we detected the concentration change of compound 23 in buffer using HPLC (High Performance Liquid Chromatography). The integral area of the compound peak represents the compound concentration in the solution. Compound 23 was dissolved first in the buffer as enzymatic assays did, then the concentration of the compound in solution was determined using HPLC with the following analytical HPLC conditions. After being treated at 37°C for 6 hours (all enzymatic assays in this study have finished within 6 hours), the concentration of compound 23 was detected again. And the buffer without compound 23 was also detected as a control. The integral area of compound 23 was 255710 in 0 h (**Figure S1B**) and 230507 in

6 h (**Figure S1C**). From the HPLC assay, no significant concentration change of compound 23 has been detected, which means compound 23 possesses the basic stability for enzymatic assays and inhibits enzymes in an intact form.

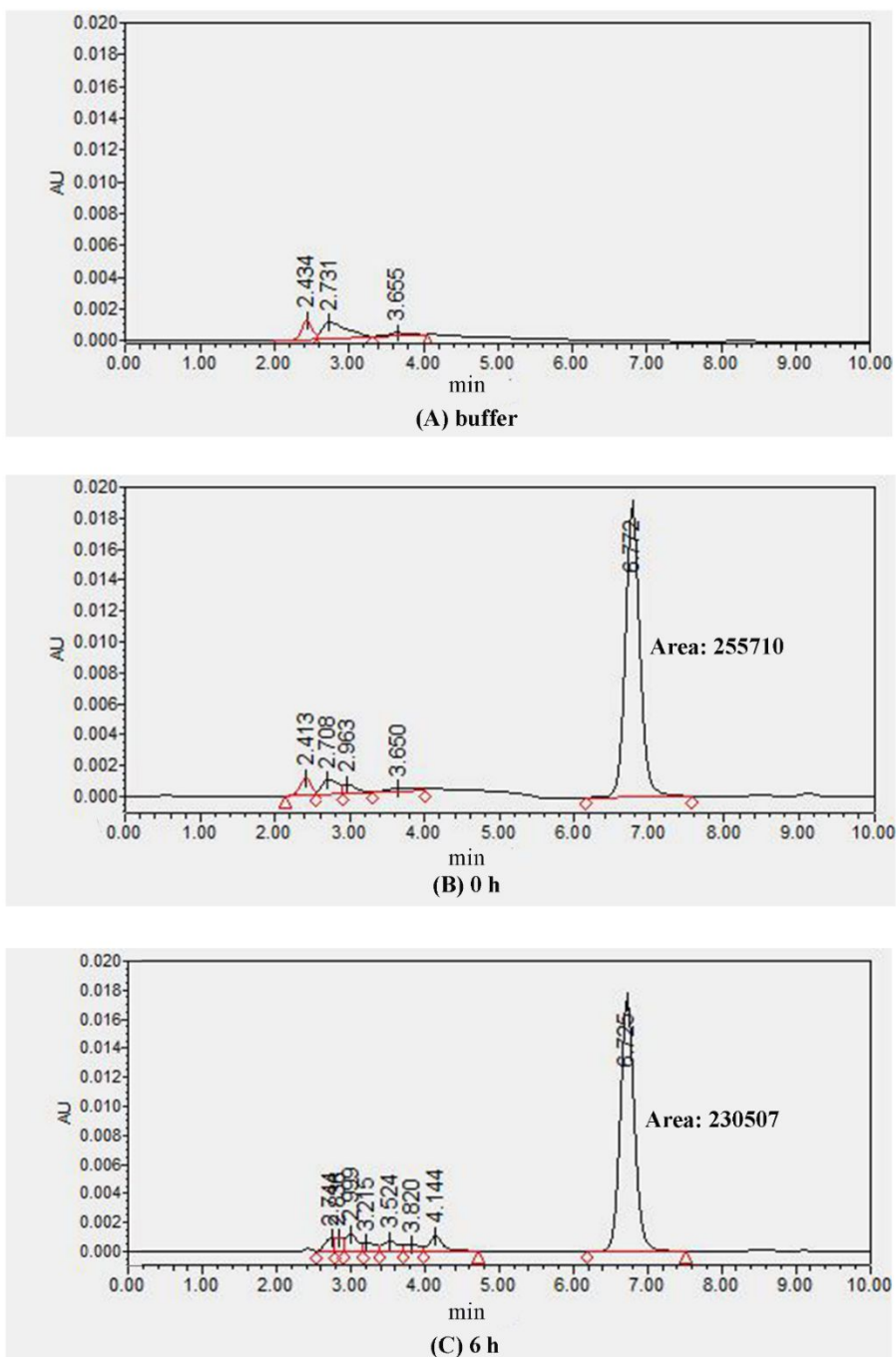


**Figure S1.** HPLC chromatogram of buffer (A), compound 23 in 0 h (B), and compound 23 in 6 h (C)

A Waters 1525 Binary Pump system with a Waters 2489 UV/Visible detector (UV detection was set to 270 nm) in series was used for high-performance liquid chromatography (HPLC). The solvent system for all HPLC measurements was A = H<sub>2</sub>O and B = methanol. Analytical HPLC condition: 85% B at a flow rate of 1 mL min<sup>-1</sup> with a Diamonsil C18 (2) 5μm 250 x 4.6mm.

### 3. Biology

#### 3.1 Inhibition rate test and IC<sub>50</sub> value determination

For inhibition rate, DENV NS2B-NS3 protease was purchased from Sino-American Biotechnology Co., Ltd. and directly used without further purification. Substrate Bz-Nle-Lys-Arg-Arg-AMC was purchased from Nanjing Peptide Biotech Ltd. and directly used without further purification. The assay buffer consisted of 1 mM CHAPS, 50 mM Tris, and 20% glycerol at pH 7.5. 30 µL of DENV NS2B-NS3 protease (final 100 nM) was distributed to a 96-well plate, and 40 µL of compounds were added followed by a 60 min incubation at 37°C temperature. The enzyme reaction was initiated by adding 30 µL of the substrate (final 3.6 µM). The fluorescence intensity was continuously monitored every min for 15 min at 37°C using a fluorimeter (Tecan Infinite F500) with 380 nm excitation and 460 nm emission wavelengths. Aprotinin was used as a positive control for every plate. All compounds were tested in triplicate. The data of fluorescence intensity versus reaction time were linearly fitted to give the slope of the function, which was used to indicate the speed of hydrolysis in the presence or absence of inhibitors. Then, the inhibition rates were calculated using the following formula:

$$\text{Inhibition rate} = \frac{S_a - S_p}{S_a} \#(1)$$

S<sub>a</sub>: the slope in the absence of inhibitor

S<sub>p</sub>: the slope in the presence of inhibitor

IC<sub>50</sub> values of optimized compounds (**20**, **22**, **23**, **32**) were measured in the same concentration of enzyme and substrate as the above inhibition rate test with a series of compound concentrations (0.16 to 40 nM). The enzyme reaction was initiated by adding 30 µL of fluorogenic substrate (final 3.6 µM), and fluorogenic signals were continuously monitored every min for 15 min at 37°C using a fluorimeter (Tecan Infinite F500) with 380 nm excitation and 460 nm emission wavelengths. Aprotinin was used as a positive control for every plate. All compounds were tested in triplicate. IC<sub>50</sub> values were calculated from plots of percent activity over compound concentration using sigmoidal dose–response by GraphPad Prism 8.

To determine the k<sub>inact</sub>/K<sub>i</sub> of compound 1 and compound 23, different concentrations of the inhibitor compound are mixed with the Bz-Nle-Lys-Arg-Arg-AMC substrate at 10 µM. The reaction was started by the addition of DENV NS2B-NS3 protease (final 50 nM). The rates were monitored over 1 h, recording the fluorescent readings at 1-minute intervals at excitation and emission wavelengths of 380 nm and 460 nm, respectively. The recorded fluorescent intensities are plotted versus time using the equation [P] = v<sub>i</sub> × (1 - exp(-k<sub>obs</sub> × t)) / k<sub>obs</sub> + d, where [P] is the product concentration, v<sub>i</sub> the initial rate, k<sub>obs</sub> the observed first-order rate constant and d is the offset. The second-order rate constant of enzyme inhibition, k<sub>inact</sub>/K<sub>i</sub>, was determined by plotting k<sub>obs</sub> versus [I] and correcting the slope with the equation k<sub>inact</sub>/K<sub>i</sub> = (1 + [S]/K<sub>m</sub>) × k<sub>obs</sub>/[I].<sup>1,2</sup>

#### 3.2 Cell line and virus

BHK-21 cells (a baby hamster kidney-derived cell line) were obtained from the Cell Bank of Type Culture Collection, Chinese Academy of Sciences. All cells were maintained in Dulbecco's modification of Eagle's medium (DMEM, Macgene) supplemented with 10% heat-inactivated fetal bovine serum (FBS, HyClone), 100 units/mL penicillin, and 100 g/mL streptomycin at 37°C in a humidified atmosphere containing 5% CO<sub>2</sub>. DENV-2 strain New Guinea C used in this study was preserved and maintained in Academy of Military Medical Sciences.

#### 3.3 Cellular protection effect assays

1.0x10<sup>4</sup> BHK-21 cells/well were seeded in 96-well plates. Each sample was repeated in 3 wells. 0.2 MOI (multiplicity of infection) of DENV virus in 100 mL DMEM (containing 2% FBS and antibiotics) were added to cells for 2 hours. Then, the virus-containing medium was removed, and the 96-well plates were washed with DMEM (containing 10% FBS). DMEM (containing 10% FBS) containing compound **23** at a concentration of 5  $\mu$ M or compound-free DMEM (containing 10% FBS) were added. After infection for 5 days, Cell viability was measured by using the CCK-8 cell counting kit (Dojindo Laboratories) according to the manufacturer's instruction. The absorbance values of compounds-treated cells and virus-infected cells were compared with the uninfected samples. The results were determined and exhibited using GraphPad Prism 8.

### 3.4 Cellular toxicity test

1.0x10<sup>4</sup> BHK-21 cells/well were seeded onto 96-well plates and treated with compound **1** or compound **23** at 5  $\mu$ M concentrations for 5 days. Cell viability of the treated cells was quantified using the CCK-8 cell counting kit (Dojindo Laboratories) according to the manufacturer's instruction. The absorbance values of compounds-treated cells were compared with normal samples. The results were determined and exhibited using GraphPad Prism 8.

## 4. Computational analyses

### 4.1 Covalent docking

The ligands in .sdf format used in molecular docking were created with ChemBioDraw Ultra and prepared by LigPrep in Schrödinger package (version 2018-4). For protein preparation, the crystal structure of DENV NS2B-NS3 (PDB code: 3U1I) was downloaded from the RCSB PDB Bank (<http://www.rcsb.org/>) and prepared by Protein Preparation Wizard in Schrödinger package (version 2018-4). All hydrogen atoms were added to residues, and all bond orders were assigned. Subsequently, the OPLS3 force field was used to minimize the protein energy and eliminate steric hindrance. For all dockings, a 10 Å × 10 Å × 10 Å grid box was generated around the active site of protein. All dockings were performed by CovDock in Schrödinger package (version 2018-4) with reactive residue setting to Ser135. Pymol (version 1.7.2.1) was used to analyze the interactions between protein and ligands.

### 4.2 Molecular dynamics simulation

The molecular dynamics simulations were applied to investigate the binding mode given by molecular docking. Multiple stages were involved in Molecular dynamics: system building, simulation, and results analysis. First, the resulting structures from the docking process were introduced into the Maestro (version 2018-4) and processed with the Protein Preparation Wizard in Schrödinger package (version 2018-4). After that, the refined structures were embedded in simple point charge (SPC) water model, and the complexes were neutralized with an appropriate number of counter ions. The system was set in an orthorhombic box, which extended approximately 10 Å in each direction. The OPLS\_3e force field was used in the protein-ligand system.<sup>3</sup> Subsequently, a minimization step was subjected to the system with the largest interaction setting to 2000 and the convergence threshold setting to 1.0 kcal/mol/Å using a hybrid method of the steepest decent and the limited-memory Broyden–Fletcher–Goldfarb–Shanno algorithms (LBFGS). The system energy was reduced to the maximum of 5000 steps until it reached the gradient threshold of 25 kcal/mol/Å. The protein-ligand systems were minimized at

a temperature of 300 K in NPT ensemble using a Nose-Hover thermostat at 300 K and Martyna-Tobias-Klein barostats at 1.01325 bar pressure. During 100 ns simulation, the energy and the trajectory of the systems were calculated and recorded every 1.2 ps and 4.8 ps, respectively. The root-mean-square deviation (RMSD), the protein-ligand interactions, and the ligand torsions of rotatable bonds were analyzed.

### 4.3 Protein contacts atlas

To investigate essential binding features and protein-ligand contacts, Protein Contacts Atlas analysis was performed by the online server at <http://www.mrc-lmb.cam.ac.uk/pca/>. The uploaded structures were extracted from MD trajectory which can represent typical interactions of the complex during simulation.<sup>4</sup>

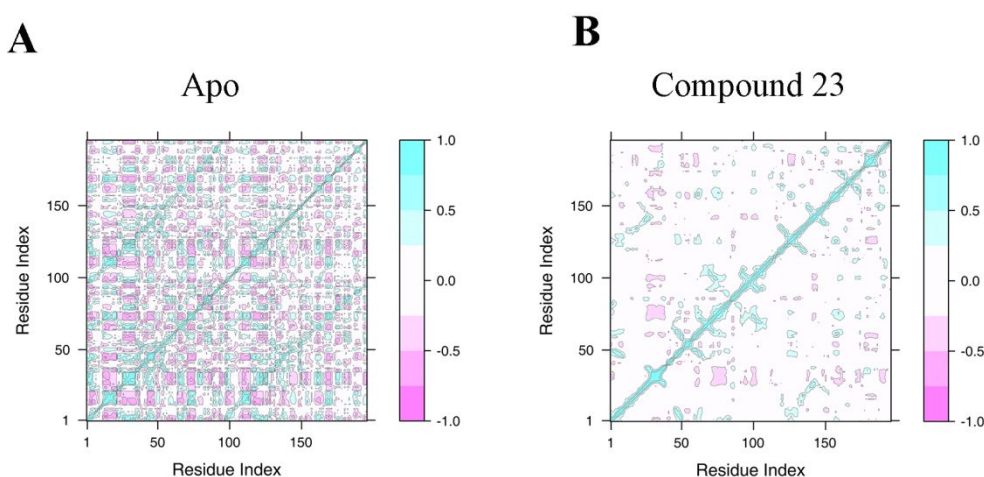
### 4.4 Dynamic cross-correlation map (DCCM)

Dynamic cross-correlation matrix (DCCM) was generated on the C- $\alpha$  atoms of the protein using the 100 ns MD trajectory with the R package Bio3D to depict the time-related motion of the complexes. The correlation coefficient  $C_{ij}$  was calculated as the following formula<sup>5</sup>:

$$C_{ij} = \frac{\langle \Delta r_i \cdot \Delta r_j \rangle}{\sqrt{\langle \Delta r_i \cdot \Delta r_i \rangle \langle \Delta r_j \cdot \Delta r_j \rangle}} \quad \#(2)$$

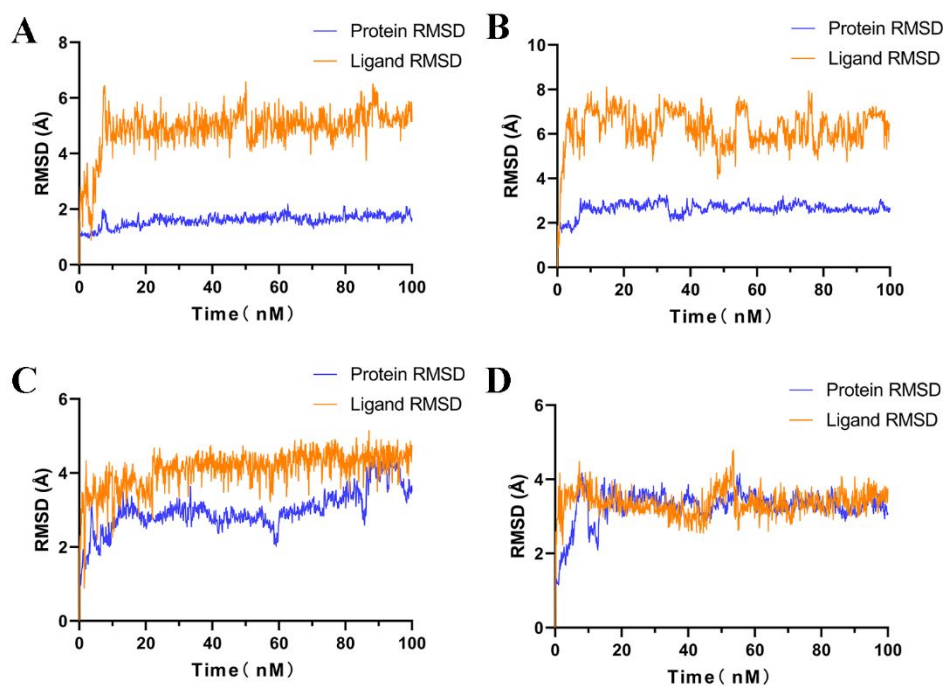
In this formula,  $\Delta r_i$  and  $\Delta r_j$  represent the displacements vector corresponding to i-th and j-th atoms. And the “ $\langle \rangle$ ” represents the ensemble average. A positively  $C_{ij}$  value means correlated motion between the i-th and j-th motion, whereas a negative  $C_{ij}$  value means inversely correlated motion between the i-th and j-th motion. The elements of the  $C_{ij}$  varied from -1 to 1<sup>6</sup>.

In order to probe the effect of compound **23** on the conformational motions of NS2B-NS3 protein, DCCM analyses were performed on all C $\alpha$  atoms in the ligand-free protein system and the protein-compound **23** complex system. As shown in **Figure S2**, the protein-compound **23** complex system showed less both correlated and anti-correlated motions which mean higher structural stability of the complex.



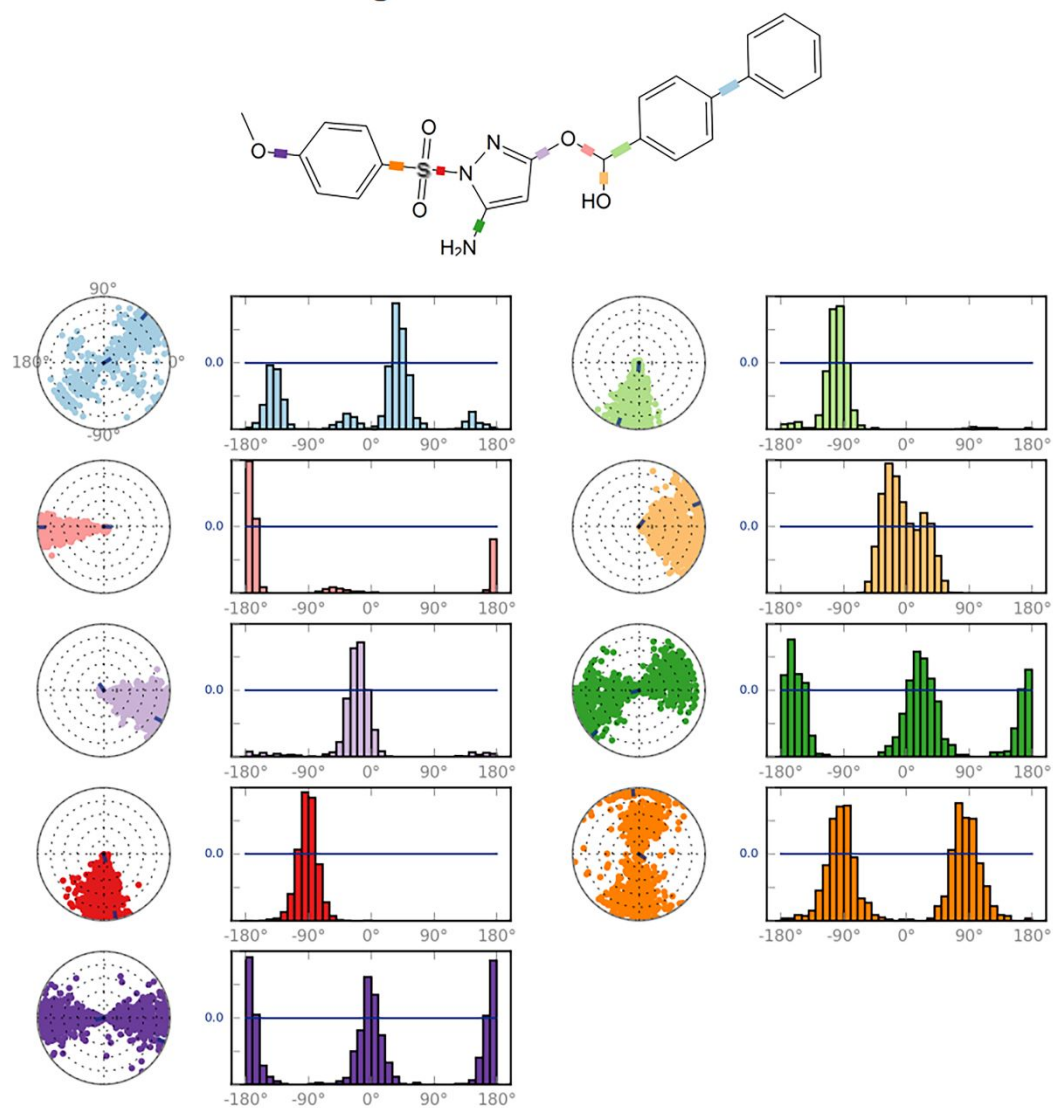
**Figure S2.** Dynamic cross-correction map (DCCM) of NS2B-NS3 Apo structure (A) and protein-compound **23** complexes (B). The positive regions (purple) indicated the strongly correlated motions of residues, while the negative regions (cyan) were associated with the anti-correlated movements.

## 5. Supplementary Figures



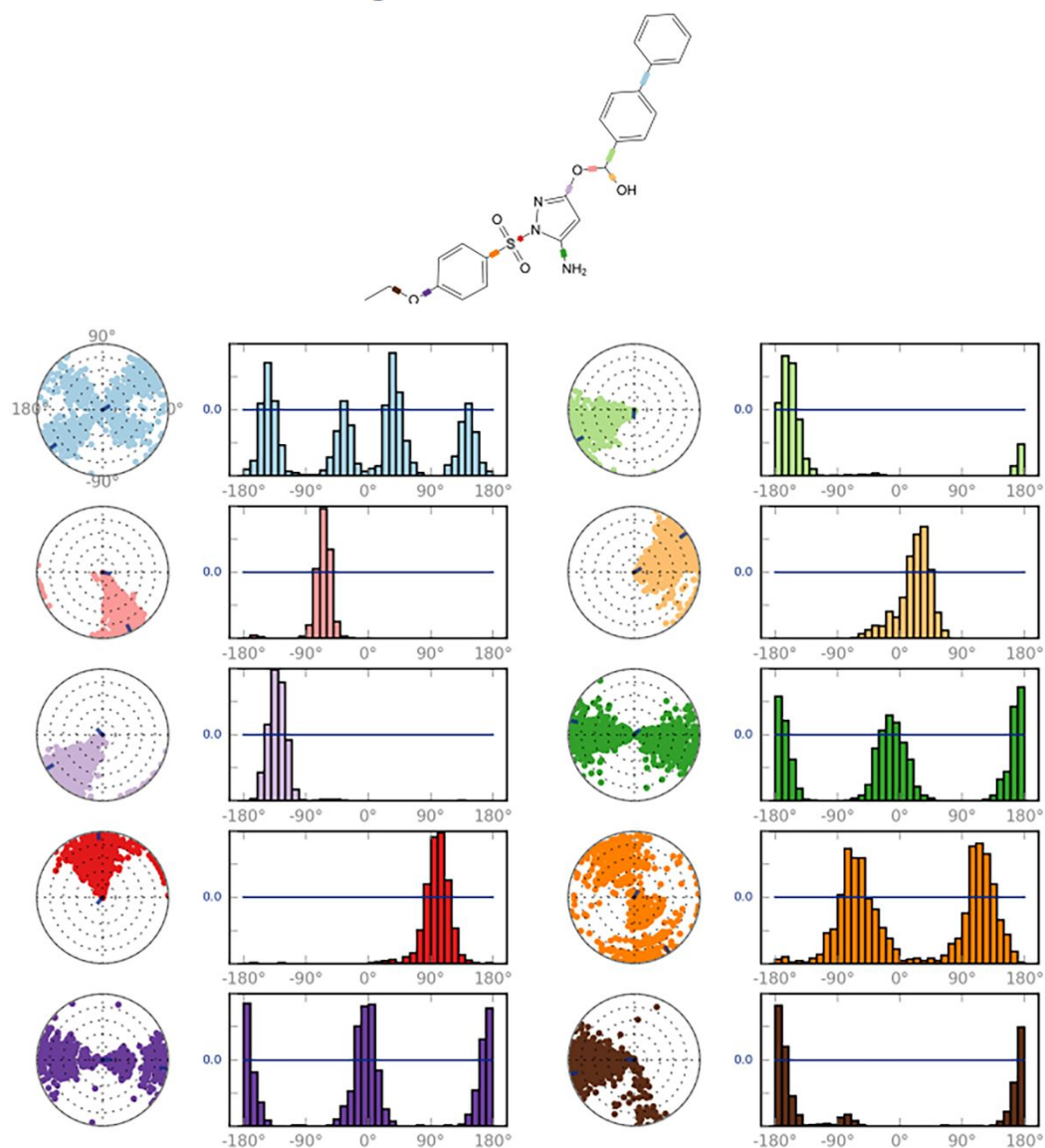
**Figure S3.** (A) RMSD of DENV NS2B-NS3 protein backbone atoms (blue line) and ligand (compound **1**) (orange line) monitored throughout the 100 ns molecular dynamics simulations. (B) RMSD of DENV NS2B-NS3 protein backbone atoms (blue line) and ligand (compound **20**) (orange line) monitored throughout the 100 ns molecular dynamics simulations. (C) MSD of DENV NS2B-NS3 protein backbone atoms (blue line) and ligand (compound **22**) (orange line) monitored throughout the 100 ns molecular dynamics simulations. (D) RMSD of DENV NS2B-NS3 protein backbone atoms (blue line) and ligand (compound **32**) (orange line) monitored throughout the 100 ns molecular dynamics simulations.

## Ligand Torsion Profile



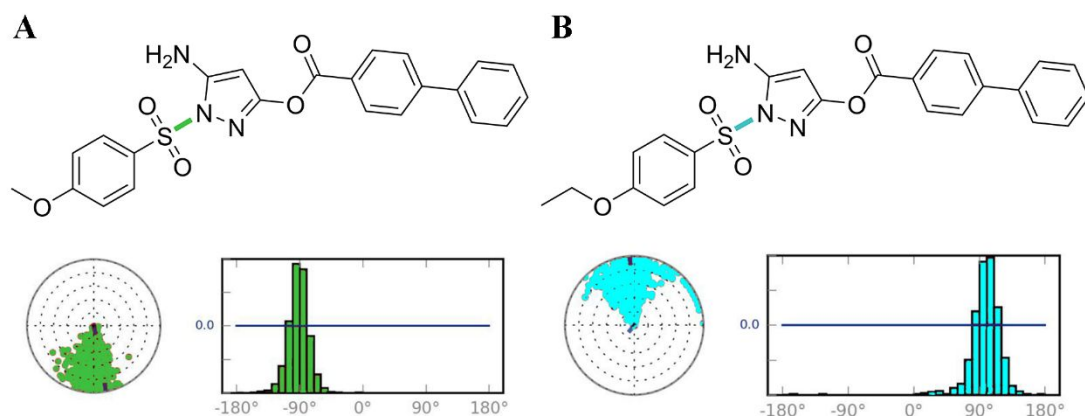
**Figure S4.** The bond torsions dial plots and bar plots of every rotatable bonds in compound 1.

## Ligand Torsion Profile



**Figure S5.** The bond torsions dial plots and bar plots of every rotatable bonds in compound 23.

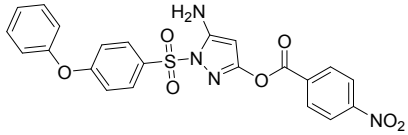
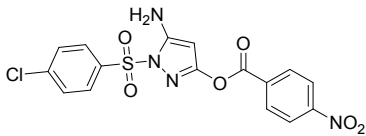
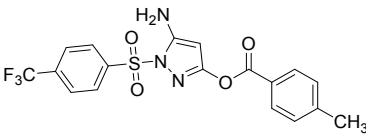
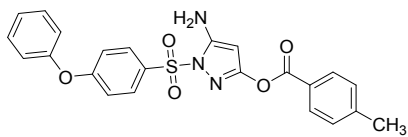
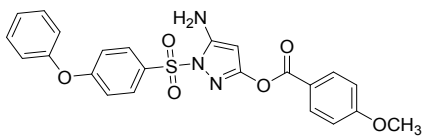
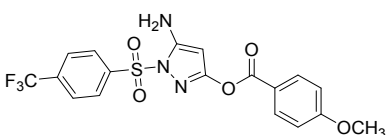
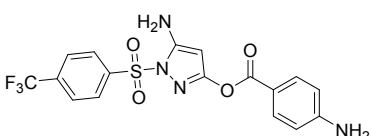
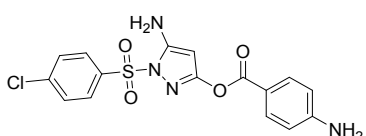
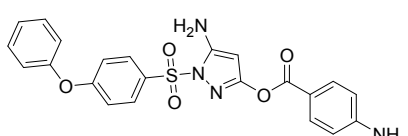
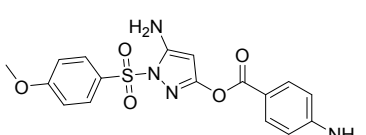


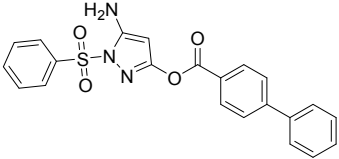
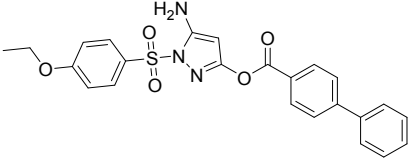
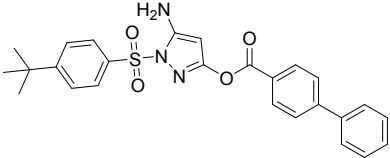
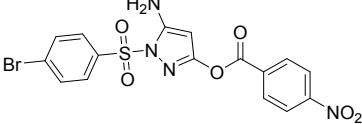
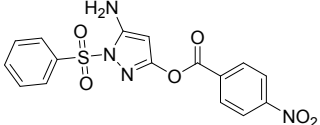
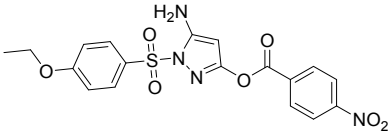
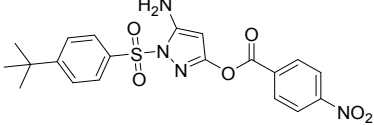
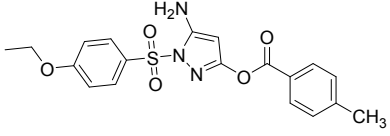
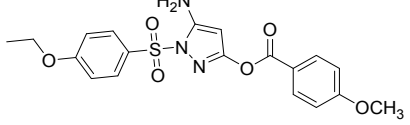
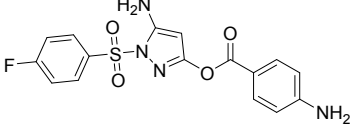


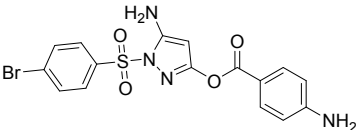
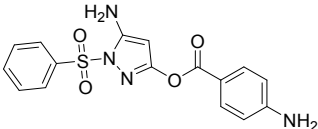
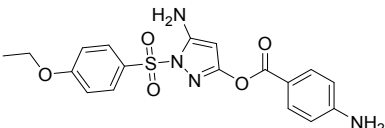
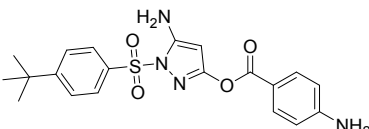
**Figure S6.** The bond torsions dial plot and bar plots of sulfonamide bond. Sulfonamide bond in (A) compound 1 (green) and (B) compound 23 (cyan). The sulfonamide bonds of compounds 1 and 23 exhibit utterly diverse directions in dynamic trajectory, indicating various binding poses of these compounds.

**Table S1.** Molecular formula, mass found and mass required.

Name	Structure	Molecular Formula	Exact Mass	ESI-MS m/z
1		$C_{23}H_{19}N_3O_5S$	449.10	450.1 [M+H] <sup>+</sup>
9		$C_{23}H_{16}F_3N_3O_4S$	487.08	488.1 [M+H] <sup>+</sup>
10		$C_{28}H_{21}N_3O_5S$	511.12	512.2 [M+H] <sup>+</sup>
11		$C_{17}H_{11}F_3N_4O_6S$	456.04	457.0 [M+H] <sup>+</sup>

12		$C_{22}H_{16}N_4O_7S$	480.07	503.0 [M+Na] <sup>+</sup>
13		$C_{16}H_{11}ClN_4O_6S$	422.01	423.0 [M+H] <sup>+</sup>
14		$C_{18}H_{14}F_3N_3O_4S$	425.07	426.1 [M+H] <sup>+</sup>
15		$C_{23}H_{19}N_3O_5S$	449.10	450.1 [M+H] <sup>+</sup>
16		$C_{23}H_{19}N_3O_6S$	465.10	466.1 [M+H] <sup>+</sup>
17		$C_{18}H_{14}F_3N_3O_5S$	441.06	442.0 [M+H] <sup>+</sup>
18		$C_{17}H_{13}F_3N_4O_4S$	426.06	427.1 [M+H] <sup>+</sup>
19		$C_{16}H_{13}ClN_4O_4S$	392.03	393.0 [M+H] <sup>+</sup>
20		$C_{22}H_{18}N_4O_5S$	450.10	451.1 [M+H] <sup>+</sup>
21		$C_{17}H_{16}N_4O_5S$	388.08	389.1 [M+H] <sup>+</sup>

22		$C_{22}H_{17}N_3O_4S$	419.09	420.1 [M+H] <sup>+</sup>
23		$C_{24}H_{21}N_3O_5S$	463.12	464.1 [M+H] <sup>+</sup>
24		$C_{26}H_{25}N_3O_4S$	475.16	476.1 [M+H] <sup>+</sup>
25		$C_{16}H_{11}BrN_4O_6S$	465.96	467.0 [M+H] <sup>+</sup>
26		$C_{16}H_{12}N_4O_6S$	388.05	389.0 [M+H] <sup>+</sup>
27		$C_{18}H_{16}N_4O_7S$	432.07	433.1 [M+H] <sup>+</sup>
28		$C_{20}H_{20}N_4O_6S$	444.11	445.1 [M+H] <sup>+</sup>
29		$C_{19}H_{19}N_3O_5S$	401.10	402.1 [M+H] <sup>+</sup>
30		$C_{19}H_{19}N_3O_6S$	417.10	418.1 [M+H] <sup>+</sup>
31		$C_{16}H_{13}FN_4O_4S$	376.06	377.0 [M+H] <sup>+</sup>

32		$C_{16}H_{13}BrN_4O_4S$	435.98	437.0 [M+H] <sup>+</sup>
33		$C_{16}H_{14}N_4O_4S$	358.07	359.0 [M+H] <sup>+</sup>
34		$C_{18}H_{18}N_4O_5S$	402.10	403.1 [M+H] <sup>+</sup>
35		$C_{20}H_{22}N_4O_4S$	414.14	415.1 [M+H] <sup>+</sup>

## References:

- (1) Breidenbach, J.; Lemke, C.; Pillaiyar, T.; Schakel, L.; Al Hamwi, G.; Dieltz, M.; Gedschold, R.; Geiger, N.; Lopez, V.; Mirza, S.; Namasivayam, V.; Schiedel, A. C.; Sylvester, K.; Thimm, D.; Vielmuth, C.; Phuong Vu, L.; Zyulina, M.; Bodem, J.; Gutschow, M.; Muller, C. E. Targeting the Main Protease of SARS-CoV-2: From the Establishment of High Throughput Screening to the Design of Tailored Inhibitors. *Angew. Chem. Int. Ed. Engl.* **2021**, *60*(18), 10423-10429. DOI: 10.1002/anie.202016961.
- (2) Li, Y.; Zhang, Z.; Phoo, W. W.; Loh, Y. R.; Li, R.; Yang, H. Y.; Jansson, A. E.; Hill, J.; Keller, T. H.; Nacro, K.; Luo, D.; Kang, C. Structural Insights into the Inhibition of Zika Virus NS2B-NS3 Protease by a Small-Molecule Inhibitor. *Structure* **2018**, *26* (4), 555-564 e553. DOI: 10.1016/j.str.2018.02.005.
- (3) Wang, Y.; Hu, B.; Peng, Y.; Xiong, X.; Jing, W.; Wang, J.; Gao, H. In Silico Exploration of the Molecular Mechanism of Cassane Diterpenoids on Anti-inflammatory and Immunomodulatory Activity. *J. Chem. Inf. Model.* **2019**, *59* (5), 2309-2323. DOI: 10.1021/acs.jcim.8b00862.
- (4) Kayikci, M.; Venkatakrishnan, A. J.; Scott-Brown, J.; Ravarani, C. N. J.; Flock, T.; Babu, M. M. Visualization and analysis of non-covalent contacts using the Protein Contacts Atlas. *Nat. Struct. Mol. Biol.* **2018**, *25*(2), 185-194. DOI: 10.1038/s41594-017-0019-z.
- (5) Chillemi, G.; D'Annessa, I.; Fiorani, P.; Losasso, C.; Benedetti, P.; Desideri, A. Thr729 in human topoisomerase I modulates anti-cancer drug resistance by altering protein domain communications as suggested by molecular dynamics simulations. *Nucleic Acids Res.* **2008**,

36 (17), 5645-5651. DOI: 10.1093/nar/gkn558.

(6) Martin, A. J.; Vidotto, M.; Boscariol, F.; Di Domenico, T.; Walsh, I.; Tosatto, S. C. RING: networking interacting residues, evolutionary information and energetics in protein structures.

*Bioinformatics* **2011**, 27(14), 2003-2005. DOI: 10.1093/bioinformatics/btr191.